Theoretical Investigation of the Spin-dependent Exciton Formation Rates in Polymeric Light-emitting Diodes

Zhigang Shuai[a]* (帥志剛), Shiwei Yin[a] (尹世偉), Liping Chen[a] (陳麗平),
Aijun Ye[b], David Beljonne[b], Jean-Luc Brédas[c]

[a]*Laboratory of Organic Solids, Center for Molecular Sciences, Institute of Chemistry,
The Chinese Academy of Sciences, 100080 Beijing, P. R. China*
[b]*Service de Chimie des Matériaux Nouveaux, Université de Mons-Hainaut,
Place du Parc 20, 7000 Mons, Belgium*
[c]*Department of Chemistry, The University of Arizona, Tucson, Arizona 85721-0041, USA*

First, a brief review is given of recent experimental and theoretical progress in the determination of the spin-dependent exciton formation rates in electroluminescent π-conjugated polymers. We then describe our recent development of the coupled-cluster equation of motion method and present its application to the theoretical study of singlet and triplet exciton formation rates and polymer light-emitting diode quantum efficiency. It is found that, in general, singlet excitons can be formed with a higher yield than triplet excitons. The underlying mechanism is still a matter of debate. Here, we explore the role of inter-chain charge-bond correlation effects.

Keywords: Coupled-cluster; Exciton formation rate; Light-emitting diodes.

INTRODUCTION

Since the discovery of electroluminescence (EL) in π-conjugated polymers by Burroughes et al.[1] in 1990, polymer-based light-emitting diodes (LEDs) have become a topic of major interest, in both industry and academia. A major motivation is the large potential market for flat display technology based on 'plastics'. From the point of view of basic research, π-conjugated polymers display fascinating electronic and electro-optic properties.

In conventional inorganic semiconductors, the intrinsic EL efficiency can be low because of high mobility and (sometimes) the presence of an indirect band gap; in the former case, the electron and hole move fast, and the probability of forming a bound state and eventually to recombine is low; in the case of indirect band gap, the electron and hole pair forms a state which is not optically allowed, and its decay to the ground state is mainly non-radiative. However, more elaborate systems such as double heterostructures lead to devices with internal efficiencies over 90%.[2] On the other hand, organic materials present key advantages related to the possibility of tailored synthesis, processability, deposition over large areas, and high emission efficiency. The π-conjugated polymers derive their semiconducting properties from their delocalized π-electron clouds along the polymer backbones, which support charge transport. In the charged state (through chemical or electrochemical doping), conjugated polymers can display high electrical conductivities at room temperature.[3]

In a typical polymer LED, the emissive polymer is sandwiched between two electrodes. The electrons and holes are injected into the emissive material and can form bound states, either singlet or triplet excitons, through Coulomb interaction. The radiative decay of the excitons gives rise to emission of photons, i.e., luminescence. The internal EL quantum efficiency can be defined as a product of three factors: $\eta_{EL} = \eta_1\eta_2\eta_3$, where η_1 is the ratio of the number of emitted photons over the number of optically active excitons; η_2 is the ratio of the number of optically active excitons over the total number of excitons; and η_3 is the ratio of the number of excitons over the number of injected charge carrier pairs. Photoluminescence (PL), the process of light emission after optical excitation is similar to the EL process; the PL quantum efficiency can be defined as $\eta_{PL} = \eta_1\eta_4$, where η_1 is the same as for EL and η_4 is the ratio of the number of optically active excitons over the number of absorbed photons due to

the photoexcitation. It has been shown that in conjugated polymers, nearly 100% of absorbed photons can give rise to excitons,[4] namely $\eta_4 \approx 100\%$.

Both electron and hole possess spin 1/2. Thus, the bound state of an electron-hole pair has spin 1 or 0. The spin 1 state consists of three microstates (triplet states) because of the 3 z-components of the spin momentum; the spin 0 state has only one microstate (singlet state). Thus, statistically upon charge injection which is normally spin un-polarized one can have three triplet states and one singlet state. Usually, in hydrocarbon systems, the triplet states do not lead to light emission due to vanishing spin-orbit coupling. Thus, on the basis of spin statistics, EL efficiency is expected to be limited to 25% of PL efficiency: $\eta_{EL} / \eta_{PL} = \eta_2 \eta_3 / \eta_4 < \eta_2$, and η_2 is the fraction of singlet excitons out of the total exciton population, one microstate out of four.

One recent breakthrough in improving organic/polymeric EL quantum efficiency is to harvest the triplet emission by using materials that have significant spin-orbit coupling, for instance, organometallic complexes[5] or dendrimers.[6] Such complexes are usually doped into wide energy gap organic hosts where balanced charge injection and efficient transport and recombination can occur. Recent work by Adachi et al. indicates that internal phosphorescence efficiency can be as high as 87%.[7] However, under the working conditions of large-area flat displays, high current densities can induce triplet-triplet annihilation, which eventually reduces light emission.

Another breakthrough is the discovery that the electrical excitation of conjugated polymers can lead to the generation of higher numbers of singlet excitons than would be expected from single spin statistics. We will briefly review some recent experimental findings and theoretical controversies on this issue in the following sections; we will then discuss our recent results based on highly correlated quantum-chemical calculations.

OVERVIEW OF EXPERIMENTAL WORK

The validity of the 25% limit on singlet excitons from spin statistics has been tested in Alq$_3$-based organic LED devices, where a singlet fraction of $(22 \pm 3)\%$ was obtained.[8] However, Cao et al. have found that for phenylene-based conjugated polymers, upon improving the electron transport presences, the ratio of external EL quantum efficiency with respect to PL can be as high as 50%.[9] Later, Ho et al. have shown that after engineering the molecular interface in polymer LEDs, the internal EL quantum efficiency can be as high

as 45%.[10] These findings have triggered much interest as well as scrutiny. Wohlgenannt et al. have designed an experimental scheme by which they are able to measure the photo-induced absorption (PA) and the photo-induced absorption-detected magnetic resonance (PADMR) in conjugated polymer thin films. The PA is usually carried out with two light beams, one to excite the sample, the other to probe the changes in transmission, i.e., $\Delta T/T$; it can detect long-lived photogenerated charge-carriers and triplet excitons.[11] The spin-dependent recombination can be studied by the spin 1/2 PADMR technique, which measures the changes (δT) in transmission modulation (ΔT) induced by the 1/2 magnetic resonance. This change is proportional to the change of population of the photo-excited species. Under saturated magnetic resonance conditions, the charge carrier (polaron) densities with parallel and antiparallel spins become equal. Thus, by measuring the changes in polaron and triplet exciton populations, the ratio of formation rates for singlet excitons over triplet excitons, $r = \dfrac{\sigma_S}{\sigma_T}$, can be determined. Wohlgennant et al. have found that: (i) the ratio r is strongly dependent on the nature of the polymeric material; and (ii) r is close to 1 for short conjugation lengths, which is in agreement with the results in Alq$_3$,[8] while r is significantly larger than 1 in extended π-systems.

Wilson et al. have recently studied the singlet/triplet ratio directly in working PLED devices, one with a platinum-containing polymer as the active layer, the other with the corresponding monomer.[13] Due to spin-orbit coupling induced by the platinum sites, the triplet states also give rise to light emission; thus, in PL and EL measurements, both triplet and singlet states can be investigated. By comparing the PL and EL efficiencies, Wilson et al. found an average singlet formation fraction of about 22% in the monomer, and on the order of 57% in the polymer. Furthermore, they found that the ratio is independent of the electric field, the temperature, and the film thickness.

Lin et al. have measured the triplet-induced absorptions with optical and electric excitations at the same singlet exciton density,[14] and they found that the singlet and triplet formation ratio is strongly dependent on the strength of the electric field, in sharp contradiction to Wilson et al. Most strikingly, they found that at low field, the ratio is much less than 25%, only at relative strong field, the ratio can be slightly higher than 25%.

Very recently, Dhoot et al. have studied the infrared absorptions of polarons and triplet excitons in a working PLED.[15] The polaron population was extracted from the field depend-

ence of the space-charge-limited current while the triplet population was measured from the triplet absorption spectrum (that was compared to the results of coupled-cluster equation-of-motion quantum-chemical calculations). Combining this information with the triplet exciton lifetime, the triplet exciton generation rate could be deduced: at low temperature, it was found that about 83% of the excitons are formed as singlets.

This short overview illustrates that the experimental results indicate a large variation in singlet formation rates, ranging from 22% to 83%. The reason behind this disparity of results is still unclear. However, it is now generally accepted that the singlet and triplet excitons can be formed at different rates and the 25% spin statistics limit can usually be overcome in conjugated polymers.

OVERVIEW OF THEORETICAL WORK

From a theoretical point of view, the observation of such high singlet exciton populations is quite intriguing. However, we recall that in the low energy scattering of neutrons and protons (both possessing spin 1/2), the cross-section for the singlet pair formation is about 20 times as large as that for the triplet state. Indeed, as noted by Wohlgenannt et al., the singlet exciton is an ionic state[12] that can be depicted as a spatially charge-separated state, while the triplet state has a mostly covalent nature in a correlated electron system and can be viewed as a spin-flip excitation. Thus, the injected charge carriers can tend to form the ionic singlet pairs, rather than covalent triplet states.

Shuai et al. have investigated the spin-dependent exciton formation cross-sections: σ_S and σ_T for singlets and triplets, respectively, to examine the possibility that singlets and triplets can form with different probabilities.[16] They applied a Fermi-Golden rule formalism to calculate the matrix elements for the exciton formation process in a coupled two-chain model. They concluded that intermolecular bond-charge correlation induces spin-dependent exciton formation rates; in model systems of polyparaphenylene vinylene (PPV), they found that singlet excitons are usually formed with a higher yield than triplet excitons. In the next section, we will briefly introduce the methodology and describe the most relevant results.[17]

Tandon, Ramasesha, and Mazumdar have developed a model based on calculations performed for two interacting hexatriene molecules, a problem that can be solved exactly.[11] Higher-lying excited states as well as the lowest exciton in both singlet and triplet manifolds have been found to be im-

portant for the charge carrier recombination processes. The importance of higher-lying excited states is strongly dependent on the bond-order alternation parameter δ: for either small δ (where the lowest excited state contributes the most) or large δ (where a higher-lying excited state dominates), the ratio r was predicted to be large, while r was found to be small in intermediate cases. They stated that the material dependence of r can be explained by the structural parameter δ. Later, in a more extended manuscript,[18] the same authors also applied a time-dependent first-order perturbation approach and concluded that the formation rate is inversely proportional to the exciton binding energy (which corresponds to the denominator in the first-order wavefunction expansion). We note that if their expression is integrated over time from 0 to infinity, the Fermi-Golden rule is recovered and the binding energy denominator becomes the Dirac-δ function, which insures energy conservation; so, the formation rate does also depend on the amount of energy to dissipate under the form of lattice vibrations, i.e., phonons.

Kobrak and Bittner[19] have simulated intrachain collision of positive and negative polarons through a mixed quantum/classical molecular dynamics approach. Due to exchange energy, the lowest triplet state lies below the lowest singlet excited state and both states lie below the free electron-hole pair state. As expected, their dynamics simulations lead to formation rates from free polaron pairs to singlet excitons that are larger than the rates for triplet exciton generation. Later, Karabunarliev and Bittner[20] have explicitly employed an electron-phonon coupling model for PPV; they derived a formulation, under the Markov approximation for one-phonon transitions, for the internal conversion rates, that is the conversion rates from the charge separated state (by assuming two charges at both ends of the chain) to the lowest singlet and triplet exciton states. They found that the rate is nearly inversely proportional to the energy separation. Thus, the ratio r can be approximated as $\dfrac{\varepsilon_T}{\varepsilon_S}$, where $\varepsilon_{T(S)}$ is the triplet (singlet) exciton binding energy. This is consistent with the first-order perturbation results of Tandon et al. when the influence of electronic coupling is neglected.[18] By employing a parameterized Hamiltonian for PPV oligomers, Karabunarliev and Bittner have found that the ratio of singlet over triplet formation rates is linearly proportional to the conjugation length, which is in qualitative agreement with the experimental findings.

Hong and Meng have provided a totally different view.[21] They suggested a so-called phonon bottleneck mechanism. Their physical picture is such that initially 25% of free carriers go to the singlet manifold and 75% go to the triplet; how-

ever, on the basis of energetic arguments, they assume that the singlets form directly into the S_1 state, while the triplets first form into a higher lying T_2 state (with T_2 close to but slightly higher in energy than S_1). In their model, the gap between T_2 and T_1 is large and forms a phonon bottleneck: namely, the T_2 state would prefer to intersystem cross to the S_1 state by spin-orbit coupling rather than decay down the triplet ladder to the T_1 bottom state. Thus, dynamically, there form more than 25% singlet states. Two points are worth noting at this stage: first, the spin-orbit coupling in hydrocarbons is usually quite weak; second, the excited state structure for the triplet manifold is usually not that simple, in the sense that a few triplet states can be present between T_1 and S_1, which would invalidate the "bottleneck" picture. We discuss below some theoretical calculations related to the electronic structure in the triplet manifold of conjugated polymers. A major result from Hong and Meng is that if the S_1/T_1 splitting is more than 0.8 eV or less than 0.3 eV, the singlet yield can be appreciably larger than 25%. Note that for many conjugated polymers and PPV specifically, the singlet-triplet splitting is around 0.7 eV.[22] Thus, according to this mechanism, the singlet and triplet exciton would form at about the same rate, in contradiction to experiment.

Thus, a clear and commonly accepted theoretical understanding has yet to appear. It is expected that both electron-electron correlation and electron-phonon coupling can play an important role. In this contribution, we will discuss the electron correlation aspects. We will first introduce our development of the coupled-cluster equation of motion approach and apply it to study the spin-dependent exciton formation rates and the description of singlet and triplet excited states.

COUPLED-CLUSTER EQUATION OF MOTION APPROACH

The coupled cluster single and double excitation (CCSD) equation of motion (EOM) approach has been shown to be accurate, efficient, and size-consistent for both the molecular ground state and low-lying excited states. It can provide the ground state, the excited states, and the charged states in a single, unified frame. We will now give a brief summary of our development of the CCSD/EOM method. Hereafter, we adopt the following convention: indices *i, j, k, l, ...* refer to occupied molecular orbitals (MOs); *a,b,c,d, ...* to virtual MOs; and *p,q,r,s,...* to generic MOs. The two-electron part is given in antisymmetric form: <pq||rs> = <pq|rs>-<pq|sr> and the two-electron integral is defined as:

$$\langle pq|rs \rangle = \iint dr_1 dr_2 \varphi_p^*(r_1)\varphi_q^*(r_2)\frac{1}{r_{12}}\varphi_r(r_1)\varphi_s(r_2) \qquad (1)$$

with φ denoting the molecular orbital (MO) wavefunction.

Ground State

The CCSD ground-state ansatz has been proposed as:[23]

$$|CC\rangle = \exp(T)|HF\rangle \qquad (2)$$

where |HF> is the HF ground-state determinant; and T consists of single and double excitations: $T = T_1 + T_2 = \sum_{ia} t_i^a a^+ i + \sum_{\substack{i>j \\ a>b}} t_{ij}^{ab} a^+ i b^+ j$, with t's being the amplitudes of the excitation configurations. The exponential ansatz by nature guarantees size-consistency. The ground-state energy and the excitation amplitudes are determined by the Schrödinger equation:

$$H|\Psi\rangle = E_{CC}|\Psi\rangle; \ H\exp(T)|0\rangle = E_{CC}\exp(T)|0\rangle \qquad (3)$$

Multiplying the latter equation by <0|, we obtain the CCSD energy expression:

$$E_{CC} = \langle 0|H\exp(T)|0\rangle = E_{HF} + \sum_{\substack{i>j \\ a>b}} \langle ij||ab\rangle (t_{ij}^{ab} + t_i^a t_j^b - t_i^b t_j^a) \ (4)$$

Multiplying Eq. (3) by $<0|i^+a$ and $<0|j^+bi^+a$ consecutively, we obtain two nonlinear equations through which the *t*-amplitudes can be solved iteratively, for instance, starting from an initial solution:

$$t_i^a = 0, \ t_{ij}^{ab} = \frac{\langle ij||ab\rangle}{\varepsilon_i + \varepsilon_j - \varepsilon_a - \varepsilon_b} \qquad (5)$$

From Eqs. (4) and (5), it is seen that the initial solution exactly corresponds to the MP2 approximation.

In order to evaluate physically measurable quantities, we also need the left eigenvector of the CCSD ground state, i.e., the so-called Λ-state in the CCSD gradient theory,[24] which is defined as:

<L₀ | = <0|(1 + Λ)exp(-T), where $\Lambda = \sum_{ia}\lambda_a^i i^+ a + \sum_{\substack{i>j \\ a>b}}\lambda_{ab}^{ij} i^+ a j^+ b$

is the de-excitation operator.

Excited States

Based on the CCSD ground state, we can establish the Heisenberg equation of motion in the Hilbert subspace, constructed by promoting one and two electrons from occupied

to virtual MOs.[25] We denote the excitation operators as μ, ν, σ, etc. The excited-state wavefunction is constructed as a linear combination of all the single and double excitations on the CCSD ground state:

$$|ex\rangle = \sum_\mu R_\mu \exp(T)|\mu\rangle \tag{6a}$$

$$\langle ex| = \sum_\mu \langle\mu|L_\mu \exp(-T) \tag{6b}$$

where $|\mu\rangle = \mu|HF\rangle$ represents an excitation determinant and R_μ is the corresponding coefficient to be determined. The excited-state Schrödinger equation becomes:

$$H|ex\rangle = E|ex\rangle; \ H\sum_\nu R_\nu \exp(T)|\nu\rangle = E\sum_\nu R_\nu \exp(T)|\nu\rangle \tag{7}$$

where E is the excited state energy. When multiplying the above equation by exp(-T) from the left and then multiplying an excitation ket configuration $\langle\mu|$, we obtain the following eigen-equation:

$$\sum_\nu \overline{H}_{\mu\nu} R_\nu = ER_\mu, \text{ where}$$

$$\overline{H} = \exp(-T)H\exp(T)$$
$$= H + [H,T] + \frac{1}{2}\big[[H,T],T\big] + \frac{1}{6}\big[[[H,T],T],T\big]$$
$$+ \frac{1}{24}\big[[[[H,T],T],T],T\big] \tag{8}$$

is the similarity transformed Hamiltonian, that is the Jacobian. The expansion terminates exactly after 5 terms, because the two-electron term of the Hamiltonian consists of 4 generic Fermion operators and each commutation with the excitation operator eliminates one generic index; thus, the last term of Eq. (8) has no generic index left and commutes with any excitation operator. In fact, in all the mathematics manipulations, the fact that all the excitation operators commute has been widely exploited.

The similarity-transformed Hamiltonian is no longer Hermitian, or under the real basis, its matrix representation is no longer symmetric. Then, corresponding to each eigenvalue, there exist a right eigenvector and a left eigenvector. The left eigenvector is expressed as:

$$\langle ex| = \sum_{\mu_1} \langle\mu|L_\mu \exp(-T) \tag{9}$$

L_μ can be determined in a similar way as for R_μ.

Positively Charged States

When an electron is ionized from a polymer chain, its

eigenstates within the CCSD-EOM approach can be constructed in the excitation space $|\sigma\rangle = \{n, g^+ no\}$, where indices *n, o* refer to occupied MOs and *g* refer to virtual MOs. Then, the eigenstates are:

$$|p\rangle = \sum_\sigma X_\sigma \exp(T)|\sigma\rangle \tag{10}$$

$$\langle p| = \sum_\sigma \langle\sigma|Y_\sigma \exp(-T) \tag{11}$$

To derive the eigen-equation, we insert Eq. (8) into the Schrödinger equation and take the coupled-cluster ground-state energy as the zero point for energy:

$$(H - E_{cc})|p\rangle = (E - E_{cc})|p\rangle \tag{12}$$

which yields

$$(H - E_{cc})\sum_\sigma X_\sigma \exp(T)|\sigma\rangle = (E - E_{cc})\sum_\sigma X_\sigma \exp(T)|\sigma\rangle \tag{13}$$

When multiplying the above equation by exp(-T) from the left and then multiplying by <σ|, we obtain the following eigen-equation:

$$\sum_\rho (\overline{H}_{\sigma\rho} - E_{CC}\delta_{\sigma\rho})X_\rho = \Delta EX_\sigma \tag{14}$$

where $\Delta E = E - E_{CC}$ is the ionization potential (IP). Similarly, we can obtain the eigen-equation for Y_σ:

$$\sum_\sigma Y_\sigma (\overline{H}_{\sigma\rho} - E_{CC}\delta_{\sigma\rho}) = \Delta EY_\rho \tag{15}$$

Hereafter, we adopt the following conventions for simplicity:

i) $f(A,B) = f(a,b) - f(b,a)$ (16a)
ii) $f(A,B,C) = f(a,b,c) + f(b,c,a) + f(c,a,b)$ (16b)
iii) $f(A,B,C,D) = f(a,b,c,d) - f(b,a,c,d)$
$$- f(a,b,d,c) + f(b,a,d,c) \tag{16c}$$

The Jacobian ($\overline{H}_{\sigma\rho}$) can be expressed within the single and double excitation space as:

$$\overline{H}_{SS} = \langle l^+ \overline{H}k\rangle$$
$$= (E_{CC} - \varepsilon_k)\delta_{lk} + \sum_{ai}\langle ki||al\rangle t_i^a + \sum_{\substack{i\\a>b}}\langle ik||ab\rangle t_{li}^{ab}$$
$$+ \sum_{abi}\langle ki||ab\rangle t_i^a t_l^b \tag{17}$$

$$\overline{H}_{SD} = \langle k^+ Hc^+ ml\rangle$$
$$= \delta_{kL}\sum_{ia}\langle iM||ac\rangle t_i^a + \langle lm||ck\rangle + \sum_a \langle ml||ac\rangle t_k^a \tag{18}$$

$$\overline{H}_{DS} = \langle l^+ m^+ cHk \rangle = \delta_{kL}\gamma(c,M) + \chi(c,k,l,m) \qquad (19)$$

where

$$\gamma(c,m) = (\varepsilon_c - \varepsilon_m)t_m^c + \sum_{ai}\langle ic\|am\rangle t_i^a + \sum_{\substack{i \\ a>b}}\langle li\|ab\rangle t_{mi}^{ab}$$

$$+ \sum_{\substack{a \\ i>j}}\langle ji\|am\rangle t_{ij}^{ac} + \sum_{abi}\langle ic\|ab\rangle t_i^a t_m^b$$

$$+ \sum_{aij}\langle ji\|am\rangle t_i^a t_j^c + \sum_{abij}\langle ji\|ab\rangle t_i^a t_{jm}^{cb}$$

$$+ \sum_{\substack{ab \\ i>j}}\langle ji\|ab\rangle t_m^a t_{ij}^{cb} + \sum_{\substack{ij \\ a>b}}\langle ji\|ab\rangle t_i^c t_{mj}^{ab}$$

$$+ \sum_{abij}\langle ji\|ab\rangle t_m^a t_j^b t_i^c$$

$$\chi(c,k,l,m) = \langle ck\|lm\rangle + \sum_i\langle ki\|lm\rangle t_i^c + \sum_a\langle ck\|aM\rangle t_L^a$$

$$+ \sum_{ai}\langle ik\|aM\rangle t_{iL}^{ac} + \sum_{a>b}\langle ck\|ab\rangle t_{lm}^{ab}$$

$$+ \sum_{ab}\langle ck\|ab\rangle t_l^a t_m^b + \sum_{ai}\langle ki\|aM\rangle t_L^a t_i^c$$

$$+ \sum_{abI}\langle Ik\|ab\rangle t_M^a t_{IL}^{cb} + \sum_{\substack{i \\ a>b}}\langle ki\|ab\rangle t_i^c t_{lm}^{ab}$$

$$+ \sum_{abi}\langle ki\|ab\rangle t_l^a t_m^b t_i^c$$

$$\overline{H}_{DD} = \langle n^+ o^+ eHd^+ ml\rangle = \delta_{ed}\delta_{nl}\delta_{om}(E_{CC} - \varepsilon_n - \varepsilon_o + \varepsilon_e)$$

$$+ \delta_{ed}\delta_{OM}\sigma(N,L) + \delta_{nl}\delta_{om}\xi(e,d) + \delta_{ed}\alpha(o,n,m,l)$$

$$+ \delta_{OM}\beta(d,N,L,e) + \sum_a\langle ml\|ad\rangle t_{no}^{ae} \qquad (20)$$

where

$$\sigma(n,l) = \sum_{ia}\langle li\|an\rangle t_i^a + \sum_{\substack{a \\ i>j}}\langle ji\|ad\rangle t_{ij}^{ae} + \sum_{abi}\langle li\|ab\rangle t_i^a t_n^b$$

$$\xi(e,d) = \sum_{ai}\langle ie\|ad\rangle t_i^a + \sum_{\substack{i \\ a>b}}\langle li\|ab\rangle t_{in}^{ab} - \sum_{aij}\langle ij\|ad\rangle t_i^a t_j^e$$

$$\alpha(o,n,m,l) = \langle ml\|on\rangle + \sum_a\langle ml\|aN\rangle t_O^a + \sum_{a>b}\langle lm\|ab\rangle t_{no}^{ab}$$

$$+ \sum_{ab}\langle ml\|ab\rangle t_o^a t_n^b$$

$$\beta(d,n,l,e) = \langle le\|dn\rangle + \sum_i\langle li\|nd\rangle t_i^e + \sum_a\langle el\|ad\rangle t_n^a$$

$$+ \sum_{ai}\langle il\|ad\rangle t_{in}^{ae} + \sum_{ai}\langle li\|ad\rangle t_n^a t_i^e$$

Within the single and double excitation space, for $S_z = 1/2$, there are six microstates, which can be linearly combined to form the spin-adapted basis. There are two vectors for $S = 3/2$, which we do not consider in this work, and four vectors for $S = 1/2$:

i) $\quad |m_\beta\rangle,$ (21a)

ii) $\quad |c_\alpha^+ m_\alpha m_\beta\rangle,$ (21b)

iii) $\quad \left(2|c_\beta^+ m_\beta l_\beta\rangle + |c_\alpha^+ m_\alpha l_\beta\rangle + |c_\alpha^+ m_\beta l_\alpha\rangle\right)\big/\sqrt{6}$

$\quad$ (with m>l), (21c)

iv) $\quad \left(|c_\alpha^+ m_\alpha l_\beta\rangle - |c_\alpha^+ m_\beta l_\alpha\rangle\right)\big/\sqrt{2}$

$\quad$ (with m>l) (21d)

The $S_z = -1/2$ spin eigenstates $|\sigma\rangle\downarrow$ is obtained by exchanging the indices α and β of eigenstates $|\sigma\rangle\uparrow$.

Negatively Charged States

When attaching an electron to a molecule, we obtain the eigenstates by using $|\nu\rangle = \{e^+, e^+ f^+ m\}$, where indices m refer to occupied MOs and e,f refer to virtual MOs. Then, the eigenstates are:

$$|n\rangle = \sum_\nu U_\nu \exp(T)|\nu\rangle, \quad \langle n| = \sum_\nu \langle\nu|V_\nu \exp(-T) \qquad (22)$$

In the same way as for the positively charged states, we can obtain the eigen-equations for U_ν and V_ν:

$$\sum_\mu (\overline{H}_{\mu\nu} - E_{CC}\delta_{\mu\nu})U_\mu = \Delta E'U_\nu \qquad (23)$$

$$\sum_\nu V_\mu(\overline{H}_{\mu\nu} - E_{CC}\delta_{\mu\nu}) = \Delta E'Y_\nu \qquad (24)$$

where $\Delta E' = E - E_{CC}$ is the electron affinity (EA).
The matrix elements for the similarity-transformed Hamiltonian $\overline{H}_{\mu\nu}$ are evaluated in the same way as in the positively charged case, which we omit here.

There are four types of $S_z = 1/2$ eigenstates $|\nu\rangle\uparrow$:

i) $\quad |e_\alpha\rangle,$ (25a)

ii) $\quad |e_\alpha^+ e_\beta^+ k_\beta\rangle,$ (25b)

iii) $\quad \left(2|e_\alpha^+ d_\alpha k_\alpha\rangle + |e_\alpha^+ d_\beta k_\beta\rangle + |e_\beta^+ d_\alpha k_\beta\rangle\right)\big/\sqrt{6}$ (d>e), (25c)

iv) $\quad \left(|e_\alpha^+ d_\beta^+ k_\beta\rangle - |e_\beta^+ d_\alpha k_\beta\rangle\right)\big/\sqrt{2}$ (d>e). (25d)

The $S_z = -1/2$ spin eigenstates $|\nu\rangle\downarrow$ is obtained by exchanging the indices α and β of eigenstates $|\nu\rangle\uparrow$.

SINGLET AND TRIPLET EXCITON FORMATION RATES IN CONJUGATED POLYMERS

We now apply the above approach to calculate the matrix elements for exciton formation rates in polymer LED structures. We suggest an interchain coupling mechanism:

Spin-dependent Exciton Formation Rates in PLEDs

J. Chin. Chem. Soc., Vol. 50, No. 3B, 2003 **697**

upon charge injection, the electrons and holes mostly migrate from one polymer chain to another. Suppose that two polymer chains are coupled, e.g., by H'. A general expression for H' (that includes both one-electron and two-electron parts) reads:

$$H' = \sum_{pq} h_{pq} p^+ q + \frac{1}{4} \sum_{pqrs} \langle pq \| rs \rangle \, p^+ q^+ sr \qquad (26)$$

Each term has a mix of chain 1 and chain 2 spin-orbital indices; h_{pq} is the hopping integral, $t^\perp$, in the MO representation:

$$h_{pq} = \sum_{\mu_1 \nu_2} t^\perp \left(\mu_1, \nu_2 \right) \Psi_{p\mu_1} \Psi_{q\nu_{21}} \quad and$$

$$\langle pq | rs \rangle = \sum_{\mu\nu\sigma\tau} \Psi_{p\mu} \Psi_{q\nu} \Psi_{r\sigma} \Psi_{s\tau} \left[\mu\sigma | \nu\tau \right]$$

Ψ is the LCAO coefficient of the one-electron wavefunction and $\left[\mu\sigma | \nu\tau \right]$ is the Coulomb integral in the site representation.

We then apply the Fermi Golden-rule to calculate the exciton formation rate: $|\langle in|H'|fi \rangle|^2 = \dfrac{\langle in|H'|fi \rangle \langle fi|H'|in \rangle}{\langle in|in \rangle \langle fi|fi \rangle}$.

Here, we focus only on the electronic tunneling factor and do not consider the energy dissipation factor. However, we note that, since the energy of the triplet state is usually lower than that of the singlet, it will be more difficult to form the triplet state since more phonons are needed, either to be released from the initial state or to be absorbed by the final state. Thus, electron-phonon interaction is expected to favor singlet for-

mation over triplet formation.

We consider a model system consisting of two PPV oligomers whose molecular planes are parallel and separated by a distance of 4 Å, see Fig. 1. Suppose that initially one chain carries a positive charge and the other a negative charge (to mimic the charge injection process in LEDs). This scenario is shown in Fig. 2, in which we only depict the singlet configuration.

The conjugated system is described by the Pariser-Parr-Pople model:

$$H = -\sum_{<\mu\nu>s} t_{\mu\nu} (c_{\mu s}^+ c_{\nu s} + h.c.) + U \sum_\mu n_{\mu\uparrow} n_{\mu\downarrow} + \sum_{\mu<\nu} V(r_{\mu\nu}) n_\mu n_\nu \quad (27)$$

The first term represents the π-electron (with spin s) hopping integral ($t_{\mu\nu}$) between nearest-neighbor carbon sites; the second and third terms are the electron-electron diagonal density-density interactions: $n_{\mu s} = c_{\mu s}^+ c_{\mu s}$, $n_\mu = \sum_s n_{\mu s}$. The long-range interactions for the π-electrons of the conjugated car-
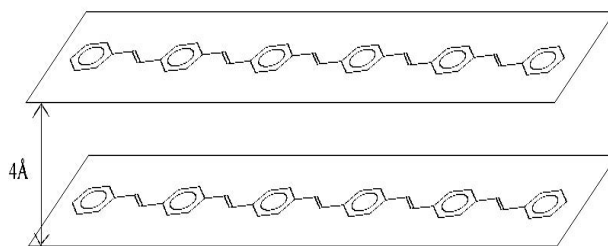
Fig. 1. Schematic configuration of two interacting PPV chains.
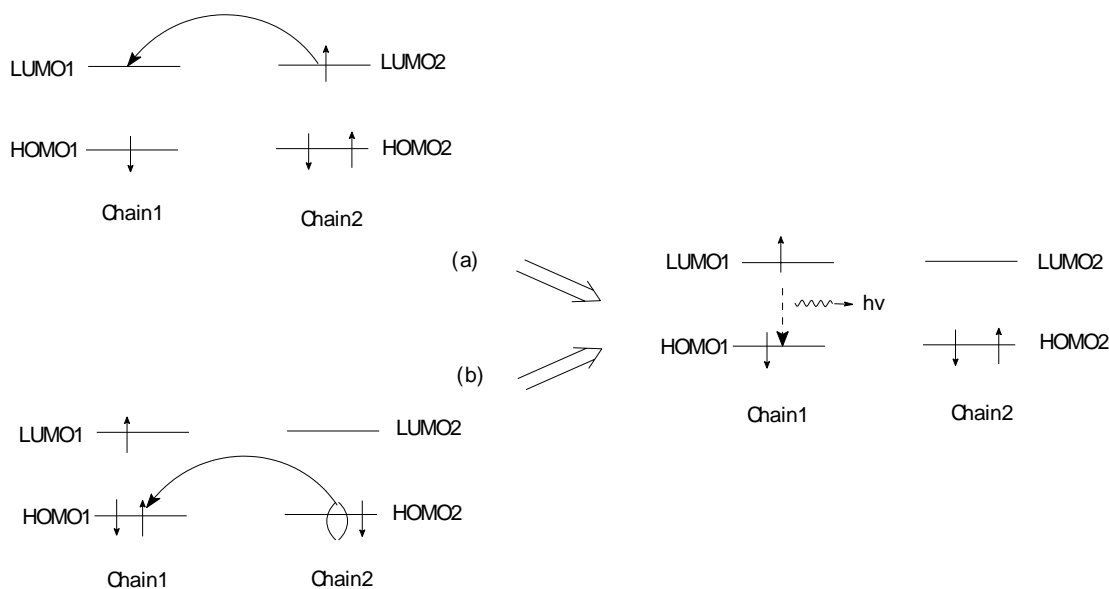
Fig. 2. Sketch of interchain charge transfer and formation of excitons.

bon systems are described by means of the Ohno-Klopman potential with U = 11.13 eV.[26]

$$V(r) = \frac{U}{\sqrt{1 + 0.5976(\varepsilon r)^2}} \qquad (28)$$

where r is the inter-nuclear distance (in Å). The Ohno-Klopman original parameters correspond to $\varepsilon = 1$. For $\varepsilon > 1$, the potential represents a more localized screened interaction. The hopping integrals are set to standard values: within the vinylene linkage, t_s = -2.2 eV for the single bonds (1.46 Å) and t_d = -2.6 eV for the double bonds (1.35 Å); in the phenylene rings, all integrals are set to t_b = -2.4 eV.

For the electronic contribution, there are two kinds of initial states and final states:

$$|in_1\rangle = \left(|n_2\rangle_\uparrow |p_1\rangle_\downarrow \pm |n_2\rangle_\downarrow |p_1\rangle_\uparrow\right)/\sqrt{2} \qquad (29a)$$

$$|in_2\rangle = \left(|p_2\rangle_\uparrow |n_1\rangle_\uparrow \pm |p_2\rangle_\downarrow |n_1\rangle_\downarrow\right)/\sqrt{2} \qquad (29b)$$

$$|fi_1\rangle = |ex_1\rangle |gs_2\rangle \qquad (29c)$$

$$|fi_2\rangle = |ex_2\rangle |gs_1\rangle \qquad (29d)$$

The ground state |gs>, negatively charged states |n>, positively charged states |p>, and exciton states |ex> are described at the CCSD/EOM level. The indices 1, 2 are for chain 1, 2; +/- is for singlet/triplet. It can be seen that <$in_1|H'|fi_1$> is the rate of exciton formed in chain 1 through electron transport, <$in_1|H'|fi_2$> is exciton formation in chain 2 through hole transport, etc. We find that for the two-body interchain coupling, the only relevant integral is of the type of [11|12] or [22|21], i.e., corresponds to interchain charge-bond interaction, denoted as X in the literature. Hereafter, we keep the dominant contributions with only one center in each chain, denoted as $X^\perp$ (μ_1, ν_2). For simplicity, we assume an exponential dependence on distance $e^{-\xi r}$ for both the $t^\perp$ and $X^\perp$ terms with ξ being chosen as reciprocal of π-orbital radius (~ 0.7 Å):

$$t^\perp \left(\mu_1, \nu_2\right) = t^\perp e^{-\zeta z(\mu_1, \nu_2)}$$

$$X^\perp \left(\mu_1, \nu_2\right) = X^\perp e^{-\zeta z(\mu_1, \nu_2)}$$

where we have assumed a long-range interaction between the two chains, and $z(\mu_1, \nu_2)$ is the distance between atom μ_1 in one chain and atom ν_2 in another chain. We treat the ratio $X^\perp/t^\perp$ as a variable.

The X-term has been found to reduce the dimerization in polyacetylene.[27] It has also been considered by Rice and Gartstein in the context of photoinduced charge transfer phenomena.[28]

We consider two limiting cases: (i) weak intermolecular

coupling: the electronic states are localized on single chains (represented by Eqs. 33a-d); and (ii) strong coupling: the electronic states are a coherent combination of the two chains.

Weak Coupling

The ratio of cross-sections for singlets and triplets in the large static disorder limit is given for electron transfer (ET) as:

$$\sigma_{S/T}^{ET} = \frac{\langle fi_{1S}|H'|in_1\rangle \langle in_1|H'|fi_{1S}\rangle}{\langle fi_{1S}|fi_{1S}\rangle \langle in_1|in_1\rangle} \Big/ \frac{\langle fi_{1T}|H'|in_1\rangle \langle in_1|H'|fi_{1T}\rangle}{\langle fi_{1T}|fi_{1T}\rangle \langle in_1|in_1\rangle} \quad (30)$$

where S/T for singlet/triplet.

Inserting (29) into (30), we obtain:

$$\langle fi_1|H'|in_1\rangle = \frac{1}{\sqrt{2}}\sum_{\mu_1\nu_2\sigma_1} L_{\mu_1}U_{\nu_{2\uparrow}}X_{\sigma_{1\downarrow}}\left\langle \mu_1^+(1+\Lambda)\overline{H}\nu_{2\uparrow}\sigma_{1\downarrow}\right\rangle$$
$$\pm L_{\mu_1}U_{\nu_{2\downarrow}}X_{\sigma_{1\uparrow}}\left\langle \mu_1^+(1+\Lambda)\overline{H}\nu_{2\downarrow}\sigma_{1\uparrow}\right\rangle \quad (31)$$

$$\langle in_1|H'|fi_1\rangle = \frac{1}{\sqrt{2}}\sum_{\mu_1\nu_2\sigma} Y_{\sigma_{1\downarrow}}V_{\nu_{2\uparrow}}R_{\mu_1}\left\langle \sigma_{1\downarrow}^+\nu_{2\uparrow}^+\overline{H}'\mu_1\right\rangle$$
$$\pm Y_{\sigma_{1\uparrow}}V_{\nu_{2\downarrow}}R_{\mu_1}\left\langle \sigma_{1\uparrow}^+\nu_{2\downarrow}^+\overline{H}'\mu_1\right\rangle \quad (32)$$

where $\overline{H}' = \exp(-T_1 - T_2)H'\exp(T_1 + T_2)$ and +/- for singlet/triplet.

Now, inserting

$$\left|\sigma_{\uparrow(\downarrow)}\right\rangle = \left\{m_{\beta(\alpha)}, double\ configuration\right\}$$

$$\left|\nu_{\uparrow(\downarrow)}\right\rangle = \left\{e_{\alpha(\beta)}^+, double\ configuration\right\}$$

$$\left|\mu\right\rangle = \left\{\left(d_\alpha^+ l_\alpha + d_\beta^+ l_\beta\right)/\sqrt{2}, double\ configuration\right\}$$

into (33) and (34), we obtain:

$$\langle fi_1|H'|in_1\rangle = C_{1L} \pm C_{3L} + Z_1 \qquad (33)$$

$$\langle in_1|H'|fi_1\rangle = C_{1R} \pm C_{3R} + Z_2 \qquad (34)$$

The Z-terms represent correlation terms due to double excitations and have a very complicated form. The C-terms are defined as:

$$C_{1L} = \sum_{med} X_m U_e L_{dm}\left(f_{d_1 e_2} + \left(\left[i_1 a_1|d_1 e_2\right] + \left[i_2 a_2|d_1 e_2\right]\right)t_i^a - \left[i_1 a_1|j_1 e_2\right]t_{i_\beta j_a}^{a_\beta d_a}\right) \quad (35a)$$

$$C_{1R} = \sum_{med} Y_m V_e R_{dm}\left(f_{d_1 e_2} + \left(\left[i_1 a_1|d_1 e_2\right] + \left[i_2 a_2|d_1 e_2\right]\right)t_i^a - \left[i_2 a_2|j_2 d_1\right]t_{i_\beta j_a}^{a_\beta e_a}\right) \quad (35b)$$

$$C_{3L} = \sum_{medl} X_m U_e L_{dl}\left(\left[l_1 d_1|m_1 e_2\right] - \left[i_1 l_1|m_1 e_2\right]t_i^a + \left[d_1 a_1|m_1 e_2\right]t_l^a \right.$$
$$\left. -\left[i_1 a_1|m_1 e_2\right]t_{i_a l_a}^{d_a a_a}\right) \quad (35c)$$

$$C_{3R} = \sum_{medl} Y_m V_e L_{dl}\left(\left[l_1 d_1|m_1 e_2\right] - \left[i_2 m_1|l_1 d_1\right]t_i^e + \left[e_2 a_1|l_1 d_1\right]t_m^a\right) \quad (35d)$$

Spin-dependent Exciton Formation Rates in PLEDs

J. Chin. Chem. Soc., Vol. 50, No. 3B, 2003 **699**

where

$$f_{a_1 b_2} = h_{a_1 b_2} + \sum_{i=i_1, i_2} \left[ii | a_1 b_2 \right]$$

$$h_{a_1 b_2} = \sum_{\mu_1 \nu_2} \Psi_{a_1 \mu_1} \Psi_{b_2 \nu_2} t^{\perp}_{\mu_1 \nu_2}$$

$$\left[i_1 j_1 | k_1 l_2 \right] = \sum_{\mu_1 \nu_2} \Psi_{i_1 \mu_1} \Psi_{j_1 \mu_1} \Psi_{k_1 \mu_1} \Psi_{l_2 \nu_2} X^{\perp}_{\mu_1 \nu_2}$$

Then, we obtain:

$$\sigma^{ET}_{S/T} = \kappa \left(\frac{C_{1L} + C_{3L} + Z_1}{C'_{1L} - C'_{3L} + Z'_1} \right) \left(\frac{C_{1R} + C_{3R} + Z_2}{C'_{1R} - C'_{3R} + Z'_2} \right) \quad (36)$$

where

$$\kappa = \left\langle ex_S | ex_S \right\rangle / \left\langle ex_T | ex_T \right\rangle$$

The C′ terms in the denominators are defined in the same way as the C terms in the numerators; the formers are evaluated with the triplet exciton wavefunction $R_\mu (L_\mu)$ and the latter with the singlet exciton wavefunction.

For hole transfer (HT):

$$\sigma^{HT}_{S/T} = \frac{\left\langle fi_{1S} | H' | in_2 \right\rangle \left\langle in_2 | H' | fi_{1S} \right\rangle}{\left\langle fi_{1S} | fi_{1S} \right\rangle \left\langle in_2 | in_2 \right\rangle} \Bigg/ \frac{\left\langle fi_{1T} | H' | in_2 \right\rangle \left\langle in_2 | H' | fi_{1T} \right\rangle}{\left\langle fi_{1T} | fi_{1T} \right\rangle \left\langle in_2 | in_2 \right\rangle} \quad (37)$$

where

$$\left\langle fi_1 | H' | in_2 \right\rangle = -C_{2L} \pm C_{4L} + Z_3$$

$$\left\langle in_2 | H' | fi_1 \right\rangle = -C_{2R} \pm C_{4R} + Z_4$$

The C terms are defined as:

$$C_{2L} = \sum_{med} X_m U_e L_{de} \left(f_{l_1 m_2} + \left(\left[i_1 a_1 | l_1 m_2 \right] + \left[i_2 a_2 | l_1 m_2 \right] \right) t^a_i + \left[i_1 a_1 | b_1 m_2 \right] t^{a_\beta b_a}_{i_\beta l_a} \right) (38)$$

$$C_{2R} = \sum_{med} Y_m V_e R_{de} \left(f_{l_1 m_2} + \left(\left[i_1 a_1 | l_1 m_2 \right] + \left[i_2 a_2 | l_1 m_2 \right] \right) t^a_i + \left[i_2 a_2 | b_2 l_1 \right] t^{a_\beta b_a}_{l_\beta m_a} \right) \quad (39)$$

$$C_{4L} = \sum_{medl} X_m U_e L_{dl} \left(\left[d_1 l_1 | e_1 m_2 \right] - \left[i_1 l_1 | e_1 m_2 \right] t^d_i + \left[d_1 a_1 | e_1 m_2 \right] t^a_l \right.$$
$$\left. - \left[i_1 a_1 | e_1 m_2 \right] t^{d_a a_a}_{i_a l_a} \right) \quad (40)$$

$$C_{4R} = \sum_{medl} Y_m V_e L_{dl} \left(\left[l_1 d_1 | e_1 m_2 \right] - \left[m_2 i_1 | l_1 d_1 \right] t^e_i + \left[a_2 e_1 | l_1 d_1 \right] t^a_m \right) \quad (41)$$

Then:

$$\sigma^{HT}_{S/T} = \kappa \left(\frac{-C_{2L} + C_{4L} + Z_3}{-C'_{2L} - C'_{4L} + Z'_3} \right) \left(\frac{-C_{2R} + C_{4R} + Z_4}{-C'_{2R} - C'_{4R} + Z'_4} \right) \quad (42)$$

$C_1(C_2)$ represents the hopping of electron (hole) from LUMO (HOMO) of chain 2 to all the virtual (occupied) orbitals of chain 1. Usually the hopping integral $t^\perp$ is negative and $X^\perp$ is positive. So, from (18), it is seen that the renormalization effect of the X-term tends to reduce $t^\perp$. C_3 and C_4 constitute pure correlation effects, which allow one to distin-

guish singlet from triplet excitations in charge transfer processes.

Strong Coupling

For strong coupling, the electronic states are coherent combinations of localized states:

$$|D_1> = (|fi_1> + |fi_2>)/\sqrt{2} \quad (43a)$$
$$|D_2> = (|fi_1> - |fi_2>)/\sqrt{2} \quad (43b)$$
$$|D_3> = (|in_1> + |in_2>)/\sqrt{2} \quad (43c)$$
$$|D_4> = (|in_1> - |in_2>)/\sqrt{2} \quad (43d)$$

(Note that $<D_1|H'|D_4> = <D_2|H'|D_3> = 0$)

In the other limiting case of delocalized excitations, the effects of electron transfer and hole transfer are coherently mixed, constructively for D_1 and destructively for D_2. The ratio of singlet/triplet formation cross-sections for Davydov states can then be expressed as:

For D_1 :

$$\sigma^{D_1}_{S/T} = \frac{\left\langle D_{1S} | H' | D_3 \right\rangle \left\langle D_3 | H' | D_{1S} \right\rangle}{\left\langle D_{1S} | D_{1S} \right\rangle \left\langle D_3 | D_3 \right\rangle} \Bigg/ \frac{\left\langle D_{1T} | H' | D_T \right\rangle \left\langle D_3 | H' | D_{1S} \right\rangle}{\left\langle D_{1T} | D_{1T} \right\rangle \left\langle D_3 | D_3 \right\rangle}$$

$$= \kappa \left(\frac{C_{1L} - C_{2L} + C_{3L} + C_{4L} + Z_1 + Z_3}{C'_{1L} - C'_{2L} + C'_{3L} + C'_{4L} + Z'_1 + Z'_3} \right)$$

$$\cdot \left(\frac{C_{1R} - C_{2R} + C_{3R} + C_{4R} + Z_2 + Z_4}{C'_{1R} - C'_{2R} + C'_{3R} + C'_{4R} + Z'_2 + Z'_4} \right)$$

For D_2 :

$$\sigma^{D_2}_{S/T} = \frac{\left\langle D_{2S} | H' | D_4 \right\rangle \left\langle D_4 | H' | D_{2S} \right\rangle}{\left\langle D_{2S} | D_{2S} \right\rangle \left\langle D_4 | D_4 \right\rangle} \Bigg/ \frac{\left\langle D_{2T} | H' | D_4 \right\rangle \left\langle D_4 | H' | D_{2T} \right\rangle}{\left\langle D_{2T} | D_{2T} \right\rangle \left\langle D_4 | D_4 \right\rangle}$$

$$= \kappa \left(\frac{C_{1L} + C_{2L} + C_{3L} - C_{4L} + Z_1 + Z_3}{C'_{1L} + C'_{2L} - C'_{3L} + C'_{4L} + Z'_1 + Z'_3} \right)$$

$$\cdot \left(\frac{C_{1R} + C_{2R} + C_{3R} - C_{4R} + Z_2 + Z_4}{C'_{1R} + C'_{2R} + C'_{3R} - C'_{4R} + Z'_2 + Z'_4} \right)$$

The expressions of $\sigma_{S/T}$ show that the cross-sections for forming singlet and triplet excitons can be very different if the interchain bond-charge correlation X is taken into account. The correlation effect for the Davydov state D_1 is much more pronounced than in the disorder case, because electron and hole contributions are constructive for the correlation terms ($C_3 + C_4$) and destructive for the mean-field terms (C_1-C_2). However, for the D_2 excited state, it is constructive for the mean-field terms ($C_1 + C_2$) and destructive for the correlation terms (C_3-C_4). Thus, the correlation effect is expected to be much less important for D_2 than D_1.

The basic reason for the X-induced spin dependent formation rate can be rationalized that the X-term in the intermolecular interaction gives rise to an exchange term in the charge transfer process. The situation is very similar to the singlet-triplet splitting, where the exchange energy plays the central role. Here, the interchain interaction determines the formation rate, thus the bond-charge correlation induced exchange term can distinguish the singlet and triplet formation processes.

For the two cases, we depict the numerical results in Fig. 3 and Fig. 4. It is observed that in the weak coupling limit, the electron transfer channel usually favors the triplet exciton formation, while hole transfer favors the singlet. For strong coupling, the two Davydov states behave very differently. Within a wide range of parameters, the triplet state for-

mation can be almost suppressed.
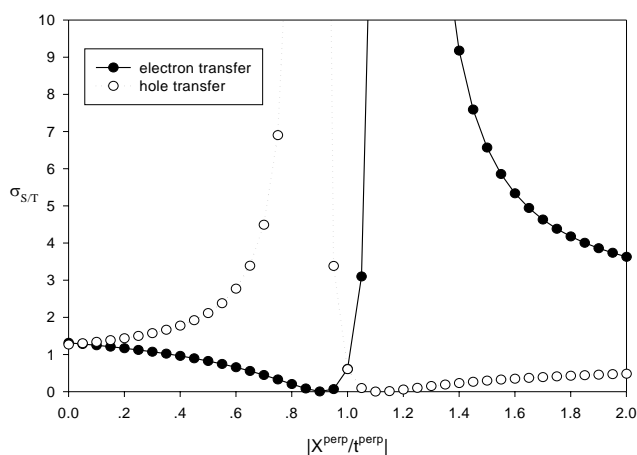
We note that even for X = 0, the ratio is not exactly 1. In fact, it is about 1.3. This is due to the fact that the wavefunctions of the singlet and triplet states have different contributions from the HOMO to LUMO transition. This is true for both the single CI and CCSD-EOM methods: roughly speaking, HOMO represents the hole level and LUMO represents the electron level.

We have also investigated the conjugation-length dependence, taking PPV oligomers as an example. We fix $X_\perp/t_\perp$ = 0.1 and calculate the formation rate as a function of the number of phenylene rings. The results are shown in Fig. 5. It is clearly seen that for the D_1 case, we find that the ratio increases with the conjugation length, in agreement with the experimental findings of Wohlgenannt et al.[12] and Wilson et al.[13]

We also note that the intermolecular bond-charge correlation is usually very small. If we suppose X = 0, as we mentioned previously, the ratio is not exactly 1. We find that in this case the ratio is strongly dependent on the on-chain electron interaction potential, see Fig. 6. It is understood that the potential form determines the nature of the singlet and triplet excitons; if the potential is short-ranged, then the HOMO $\rightarrow$ LUMO contribution is lessened. In Fig. 7, we illustrate the singlet and triplet formation rates as a function of the potential range: the larger the parameter ε, the shorter the potential range.

We also briefly mention that in the CCSD/EOM approach, an approximation in calculating the excited state is to restrict the configuration space to single excitations, while keeping the ground state as CCSD. In principle, this is a

Fig. 3. Ratio of singlet to triplet exciton formation rates as a function of X/t: weak coupling.

Fig. 4. Ratio of singlet to triplet exciton formation rates as a function of X/t: strong coupling.
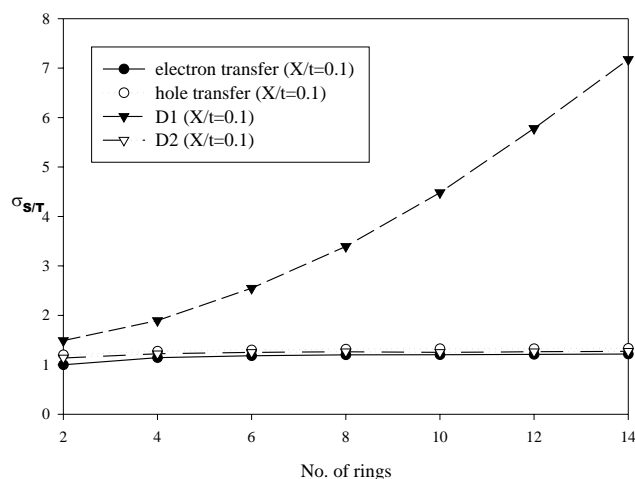
Fig. 5. Chain-length dependence of the $\sigma_{S/T}$ ratio for the four cases discussed in the text.

Spin-dependent Exciton Formation Rates in PLEDs

J. Chin. Chem. Soc., Vol. 50, No. 3B, 2003   **701**
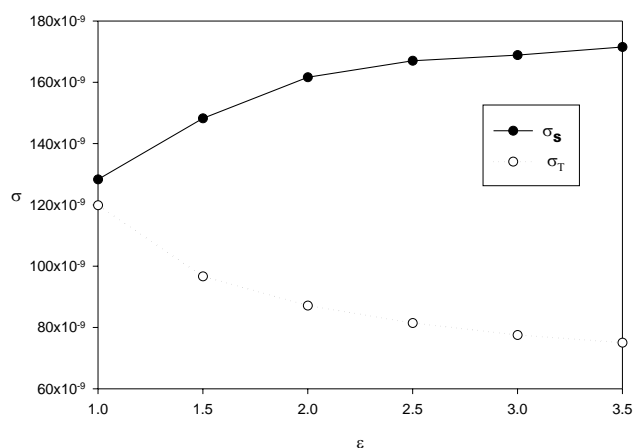
Fig. 6. Formation rates as a function of the potential parameter: the larger ε, the shorter the interaction range.
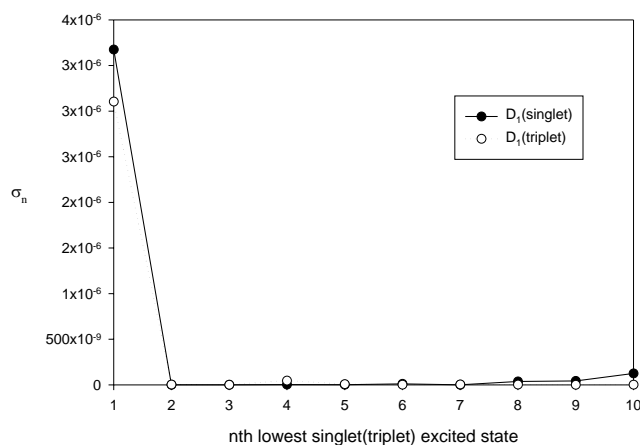
Fig. 7. Formation rates for different excited states.
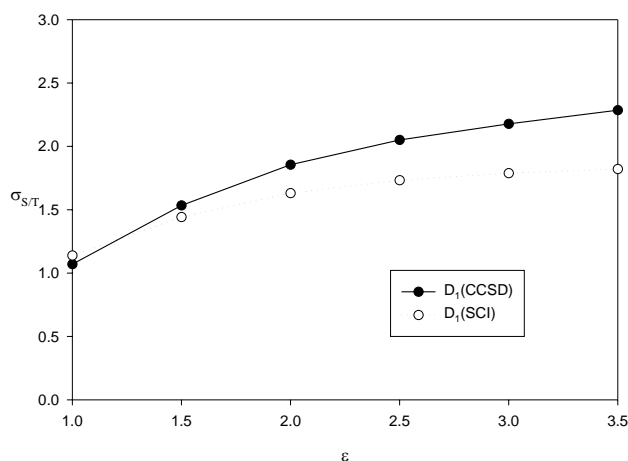
Fig. 8. Comparison of CCSD with SCI for the ratio of the singlet-triplet formation rate for different

better approach than either the Random Phase Approximation (RPA) or single configuration interaction (SCI), since the ground state is highly correlated (in RPA, there exists a double counting problem for the ground state in evaluating its characteristics, while for SCI, there is no correlation at all for the ground state). This approach, referred to as CCS/EOM is highly efficient (as fast as SCI or RPA) and based on the (correct) CCSD ground state. Indeed, when comparing the results of exciton formation rates based on both CCSD/EOM and CCS/EOM methods, we only find minor differences, see Fig. 8. Thus, we believe that for the description of large molecular systems, the CCS/EOM is a method of choice for evaluating the excited states.

SUMMARY

We have reviewed recent experimental and theoretical developments on the spin-dependent exciton formation rates in organic molecular and polymeric light-emitting materials. We have described our development of the CCSD/EOM method for the excited states and charged states. We have applied this method to study the exciton formation rates in conjugated polymers and found that electron correlation effects, namely the interchain bond-charge correlation terms, favor singlet exciton formation in most cases.

We stress, however, that these conclusions are based on the sole consideration of the matrix elements to form the lowest singlet and triplet excited species. We are now extending our model to account for the possibility of generation of higher lying singlet and triplet states and the release of excess energy under the form of phonons emission.[29]

REFERENCES

1. (a) Burroughes, J. H.; Bradley, D. D. C.; Brown, A. R.; Marks, R. N.; Mackay, K.; Friend, R. H.; Burn, P. L.; Holmes, A. B. *Nature (London)* **1990**, *347*, 539. (b) Gustafsson, G.; Cao, Y.; Treacy, G. M.; Klavetter, F.; Colaneri, N.; Heeger, A. J. *Nature (London)* **1992**, *357*, 477.

2. Schnitzer, I.; Yablonovitch, E.; Caneau, C.; Gmitter, T. J. *Appl. Phys. Lett.* **1993**, *63*, 131.

3. Shirakawa, H.; Louis, E. J.; MacDiarmid, A. G.; Chiang, C. K.; Heeger, A. J. *Chem. Comm.* **1977**, 578.

4. Harrison, N. T.; Hayes, G. R.; Phillips, R. T.; Friend, R. H. *Phys. Rev. Lett.* **1996**, *77*, 1881.

5. Baldo, M. A.; Thompson, M. E.; Forrest, S. R. *Nature (London)* **2000**, *403*, 750.

6. Lo, S. C.; Male, N. A. H.; Markham, J. P. J.; Magennis, S. W.; Burn, P. L.; Salata, O. V.; Samuel, I. D. W. *Adv. Mater.* **2002**, *14*, 975.

7. Adachi, C.; Baldo, M. A.; Thompson, M. E.; Forrest, S. R. *J. Appl. Phys.* **2001**, *90*, 5048.

8. Baldo, M. A.; O'Brien, D. F.; Thompson, M. E.; Forrest, S. R. *Phys. Rev. B* **1999**, *60*, 14422.

9. Cao, Y.; Parker, I. D.; Yu, G.; Zhang, C.; Heeger, A. J. *Nature (London)* **1999**, *397*, 414.

10. Ho, P. K. H.; Kim, J.; Burroughes, J. H.; Becker, H.; Li, S. F. Y.; Brown, T. M.; Cacialli, F.; Friend, R. H. *Nature (London)* **2000**, *404*, 481.

11. Wohlgenannt, M.; Tandon, K.; Mazumdar, S.; Ramasesha, S.; Vardeny, Z. V. *Nature (London)* **2001**, *409*, 494.

12. Wohlgenannt, M.; Jiang, X. M.; Vardeny, Z. V.; Janssen, R. A. J. *Phys. Rev. Lett.* **2002**, *88*, 197401.

13. Wilson, J. S.; Dhoot, A. S.; Seeley, A. J. A. B.; Khan, M. S.; Köhler, A.; Friend, R. H. *Nature (London)* **2001**, *413*, 828.

14. Lin, L. C.; Meng, H. F.; Shy, J. T.; Horng, S. F.; Yu, L. S.; Chen, C. H.; Liaw, H. H.; Huang, C. C.; Peng, K. Y.; Chen, S. A. *Phys. Rev. Lett.* **2003**, *90*, 036601.

15. Dhoot, A. S.; Ginger, D. S.; Beljonne, D.; Shuai, Z.; Greenham, N. C. *Chem. Phys. Lett.* **2002**, *360*, 195.

16. Shuai, Z.; Beljonne, D.; Silbey, R. J.; Brédas, J. L. *Phys. Rev. Lett.* **2000**, *84*, 131.

17. Ye, A.; Shuai, Z.; Brédas, J. L. *Phys. Rev B* **2002**, *65*, 045208.

18. Tandon, K.; Ramasesha, S.; Mazumdar, S. *Phys. Rev. B* **2003**, *67*, 045109.

19. Kobrak, M. N.; Bittner, E. R. *Phys. Rev. B* **2000**, *62*, 11473.

20. Karabunarliev, S.; Bittner, E. R. *Phys. Rev. Lett.* **2003**, *90*, 079901.

21. Hong, T.; Meng, H. *Phys. Rev. B* **2001**, *63*, 1.

22. Beljonne, D.; Shuai, Z.; Friend, R. H.; Brédas, J. L. *J. Chem. Phys.* **1995**, *102*, 2042.

23. (a) Cizek, J. *J. Chem. Phys.* **1966**, *45*, 4256. (b) Cizek, J.; Paldus, J. *Phys. Scr.* **1980**, *21*, 251. (c) Bartlett, R. J. *Annu. Rev. Phys. Chem.* **1981**, *32*, 359. (d) Purvis III, G. D.; Bartlett, R. J. *J. Chem. Phys.* **1982**, *76*, 1910. (e) Bartlett, R. J. *J. Phys. Chem.* **1989**, *93*, 169.

24. Scheiner, A. C.; Scuseria, G. E.; Rice, J. E.; Lee, T. J.; Schaefer, H. F. *J. Chem. Phys.* **1987**, *87*, 5361.

25. (a) Stanton, J. F.; Bartlett, R. J. *J. Chem. Phys.* **1989**, *98*, 7029. (b) Monkhorst, H. J. *Int. J. Quantum Chem. Symp.* **1984**, *18*, 255. (c) Shuai, Z.; Brédas, J. L. *Phys. Rev. B* **2000**, *62*, 15452.

26. (a) Ohno, K. *Theor. Chim. Acta* **1964**, *2*, 219. (b) Klopman, G. *J. Am. Chem. Soc.* **1964**, *86*, 4550.

27. Campbell, D. K.; Gammel, J. T.; Loh, Jr. E. Y. *Phys. Rev. B* **1990**, *42*, 475.

28. Rice, M. J.; Gartstein, Yu. N. *Phys. Rev. B* **1996**, *53*, 10764.

29. Beljonne, D.; Ye, A.; Shuai, Z.; Brédas, J. L. submitted for publication.